Supplement for paper Large-scale circulation and stratocumulus variability

1 Coherence for each stratocumulus (Sc) region

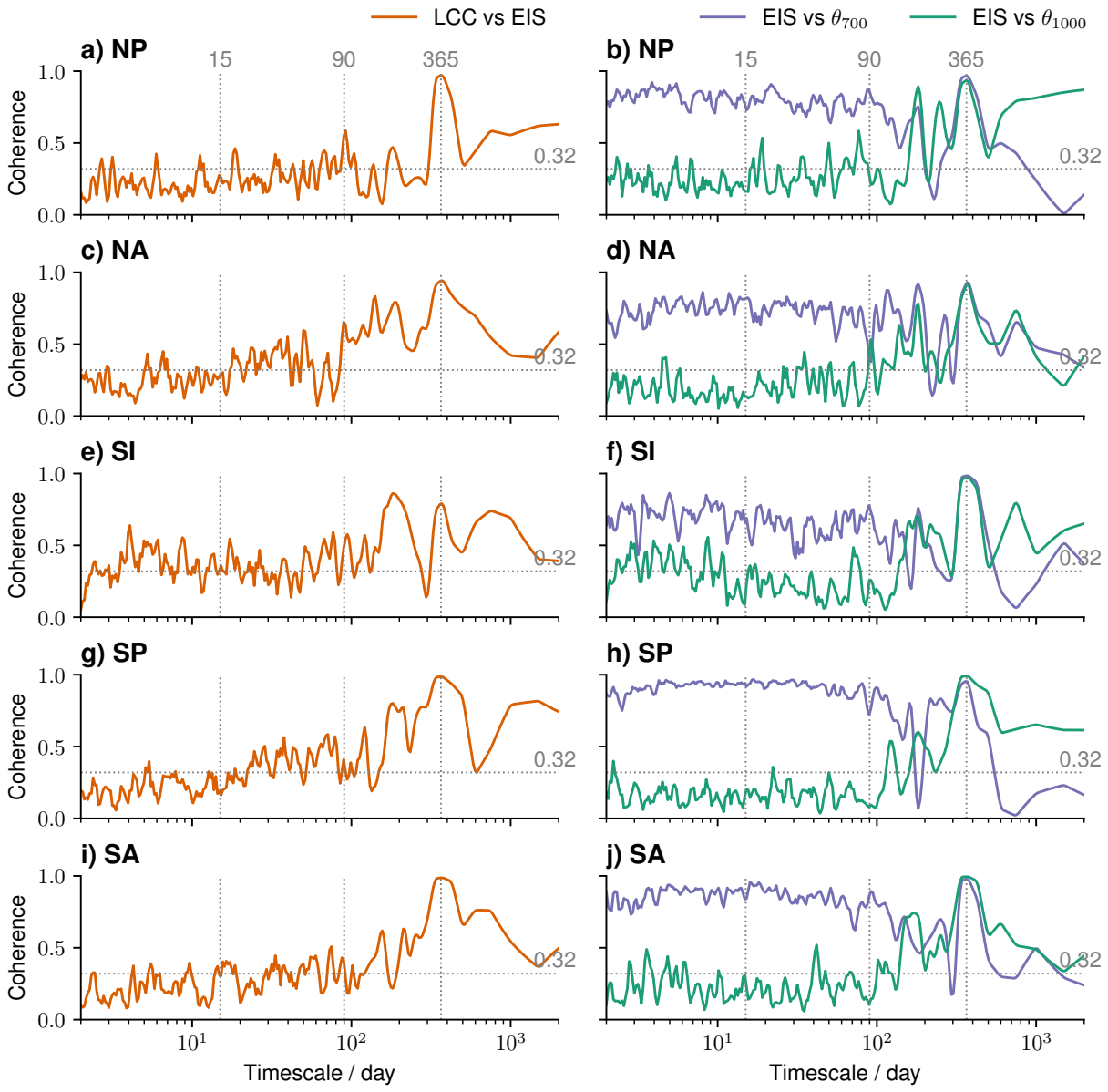

Figure S1: Left: coherence of LCC versus EIS across timescales. Right: coherence of EIS versus $\theta_{700}/\theta_{1000}$ across timescales. NP: North Pacific Sc area. NA: North Atlantic Sc area. SI: South Indian Ocean Sc area. NP: South Pacific Sc area. SA: South Atlantic Sc area.

2 Deseasonalized LCC variance across Timescales from fast Fourier transform

Table S1: Variance of LCC on each timescales after deseasonalization (derived from the fast Fourier transform).

	$\sigma^2_{\text{synoptic}}$	$\sigma^2_{\text{subseasonal}}$	$\sigma^2_{\text{interseasonal}}$	$\sigma^2_{\text{interannual}}$
North Pacific (NP)	136	137	34	24
North Atlantic (NA)	204	187	51	19
South Indian Ocean (SI)	130	86	21	16
South Pacific (SP)	46	48	14	12
South Atlantic (SA)	65	60	13	13

3 Dominant wavenumbers for EIS variability

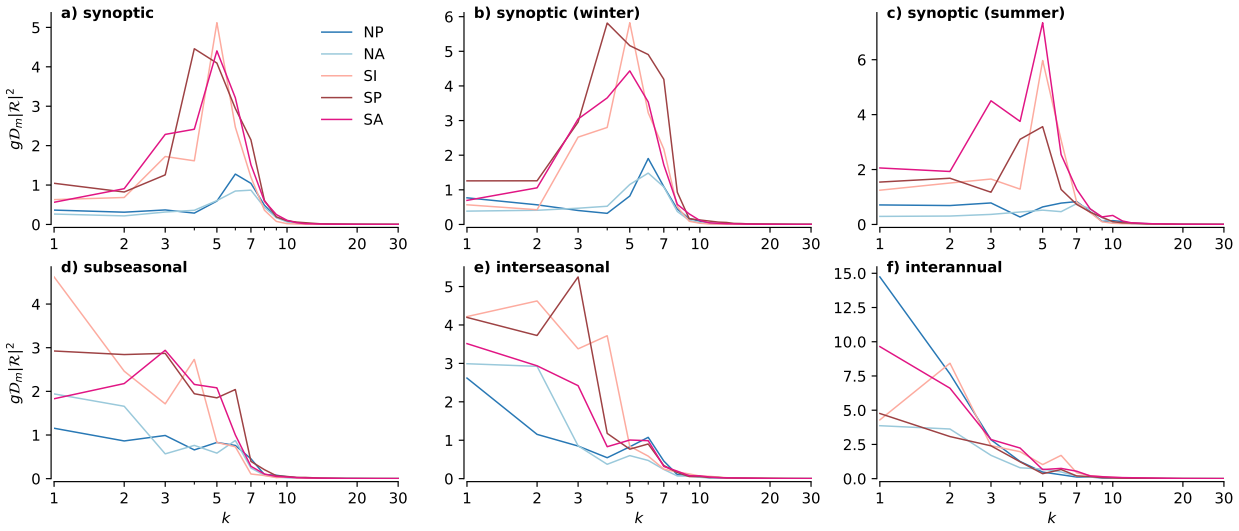

Figure S2: Variance ($g\mathcal{D}_m|\mathcal{R}|^2$) of Rossby modes coupled with EIS as a function of zonal wavenumber (k). Each color represents a region, g denotes gravity, and $\mathcal{D}_m$ denotes equivalent depth on the vertical dimension.

4 Regression results for an open-ocean area in North Pacific

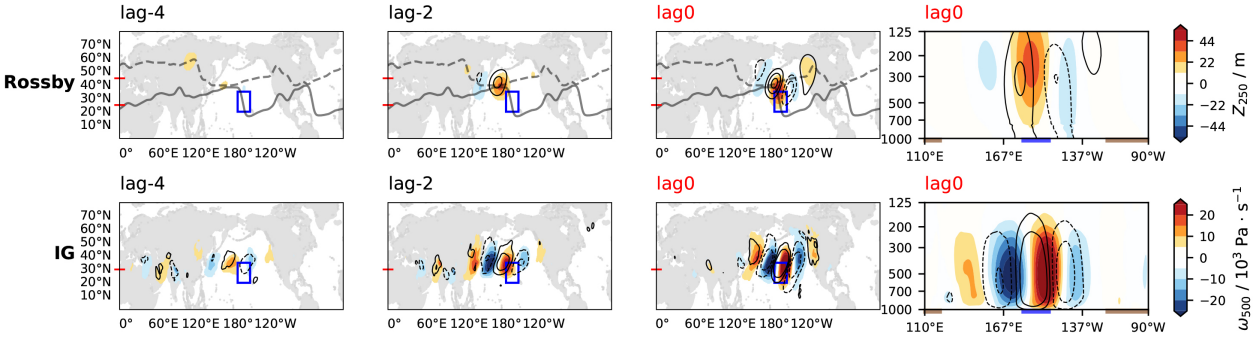

Figure S3: Synoptic timescales plots. Visualization settings are similar to Figures 3 and 4 in the paper but for regressions in an open-ocean area marked by the blue box.

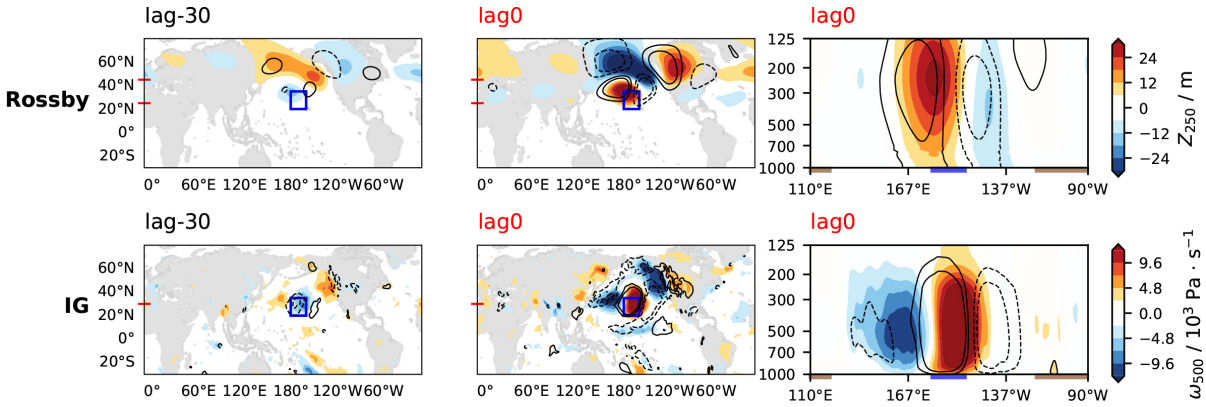

Figure S4: Subseasonal timescales plots for the open-ocean area (blue box).

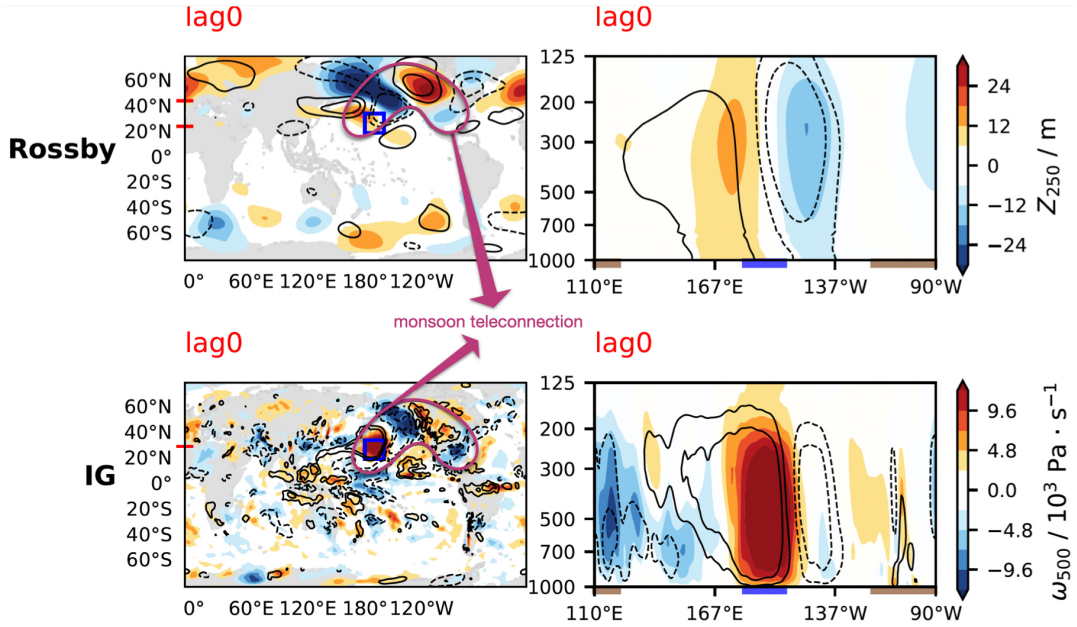

Figure S5: Interseasonal timescales plots for the open-ocean area (blue box).

5 Composite results for an open-ocean area in North Pacific

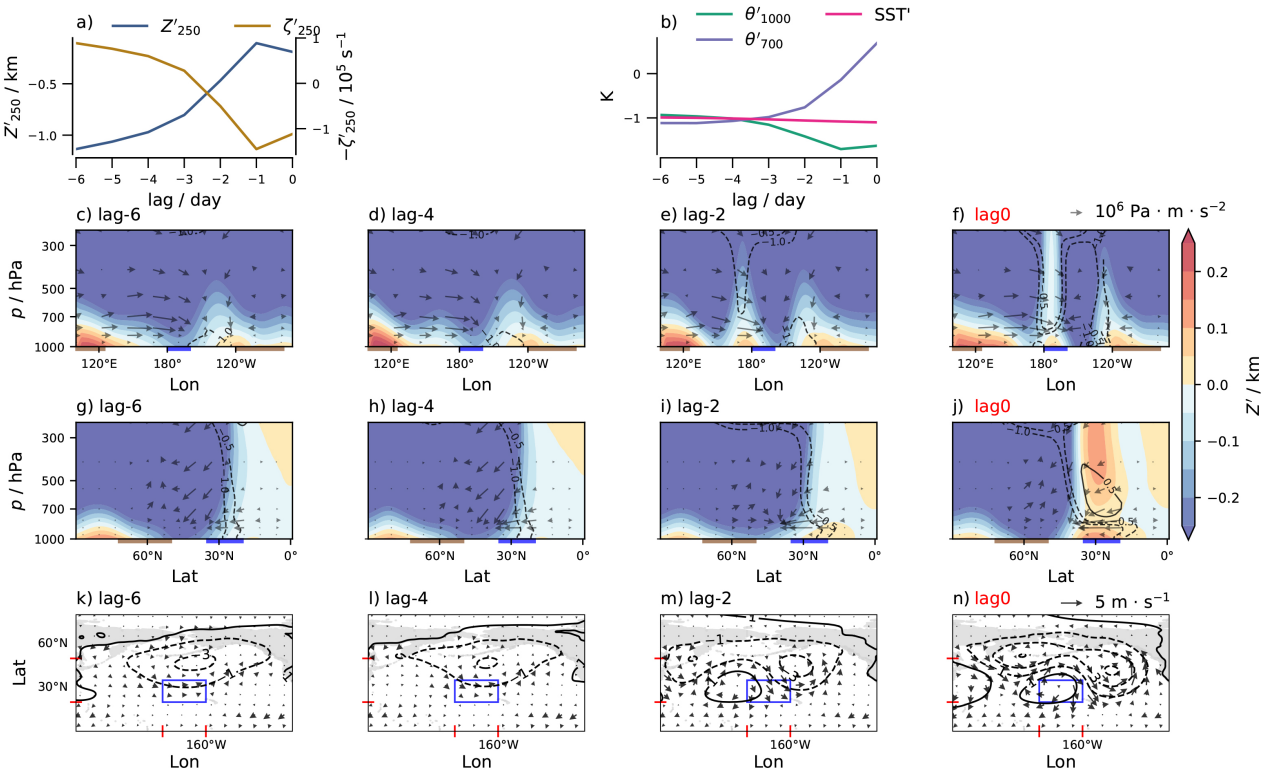

Figure S6: Similar to Figure 8 in the paper but for the open-ocean area.

6 Winter and summer patterns on synoptic timescales

Rossby modes:

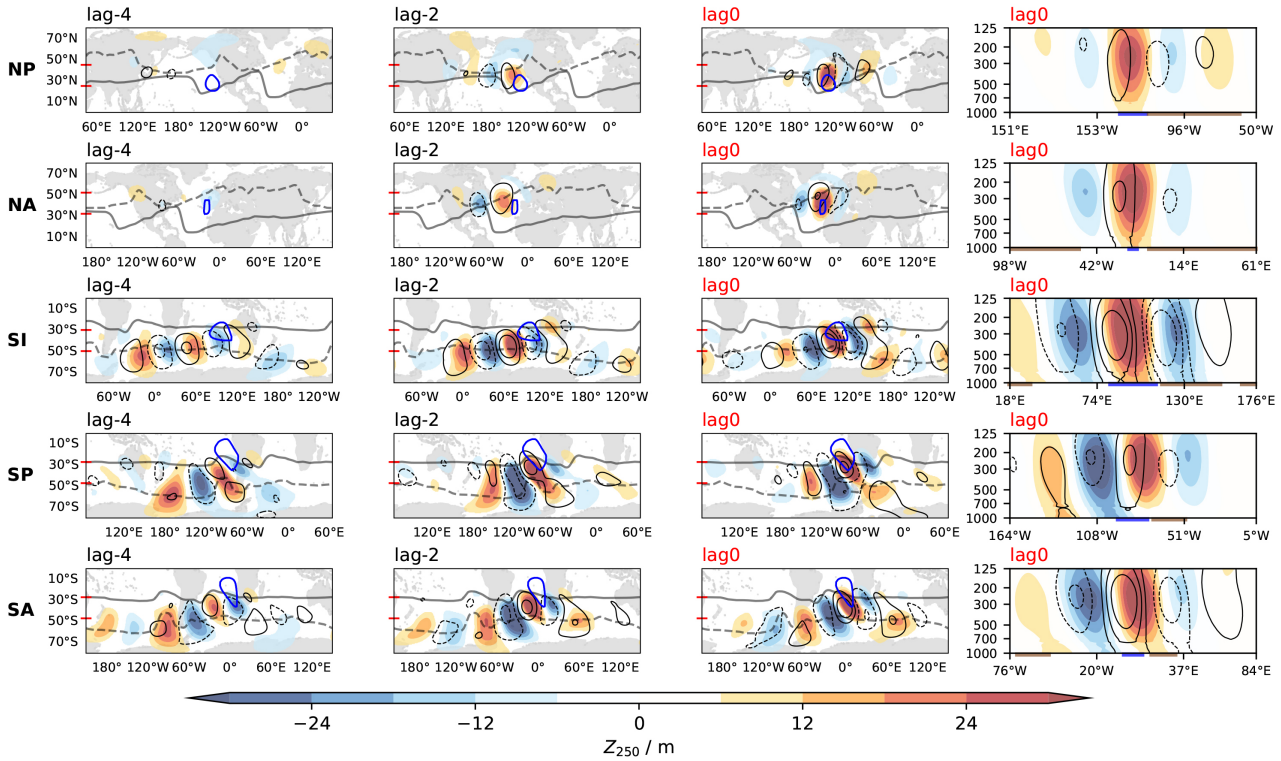

Figure S7: Winter (DJF for the Northern hemisphere and JJA for the Southern hemisphere) version of Figure 3 in the paper.

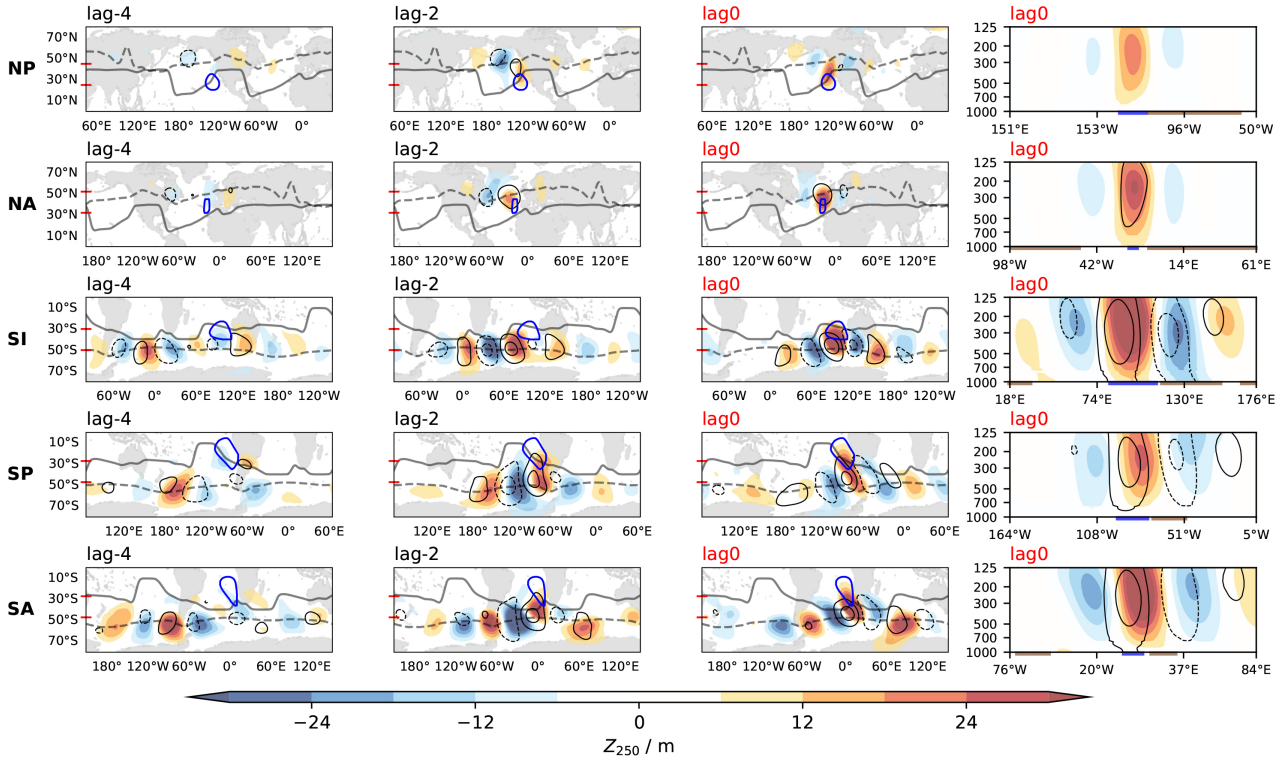

Figure S8: Summer (JJA for the Northern hemisphere and DJF for the Southern hemisphere) version of Figure 3 in the paper.

IG modes:

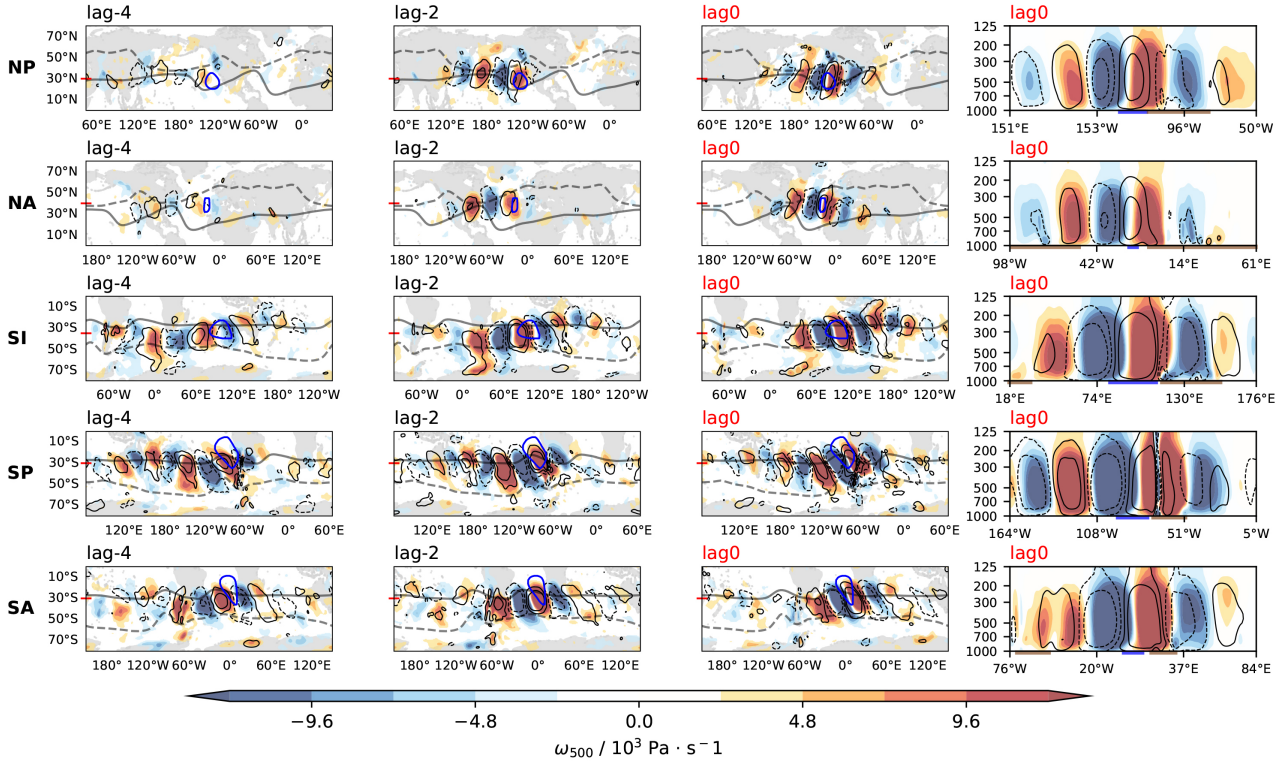

Figure S9: Winter version (DJF for the Northern hemisphere and JJA for the Southern hemisphere) of Figure 4 in the paper.

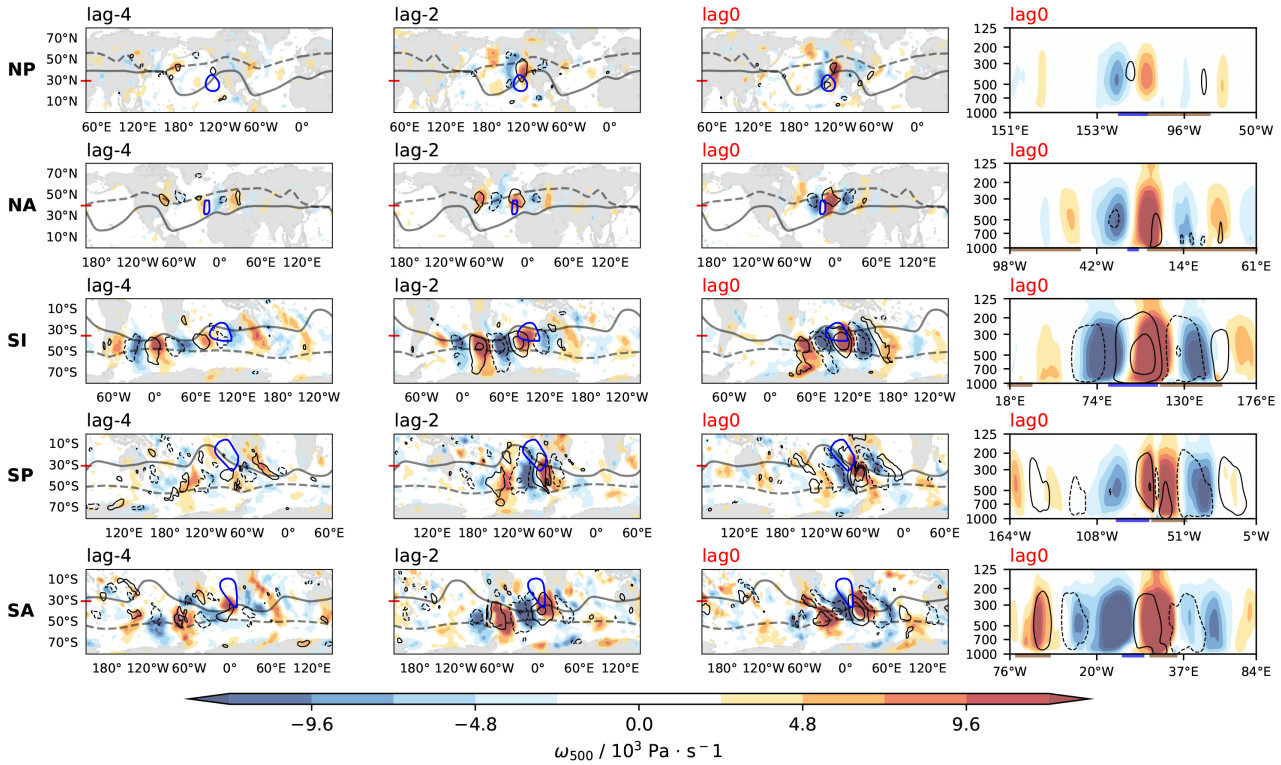

Figure S10: Summer (JJA for the Northern hemisphere and DJF for the Southern hemisphere) version of Figure 4 in the paper.

7 Subseasonal Rossby modes for all regions

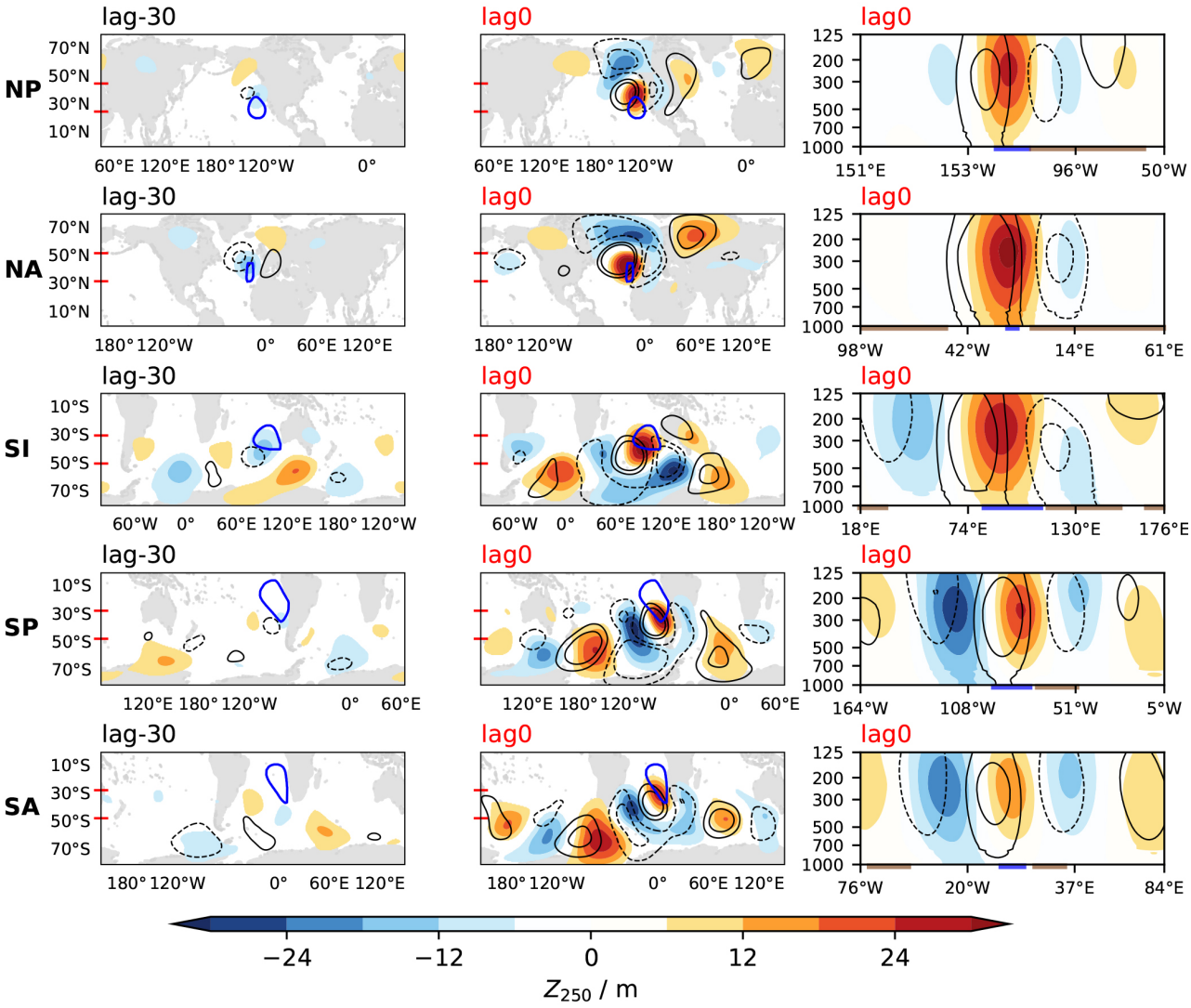

Figure S11: Similar to Figure 5 in the paper but only show Rossby modes for all regions.

8 Interseasonal patterns for all regions

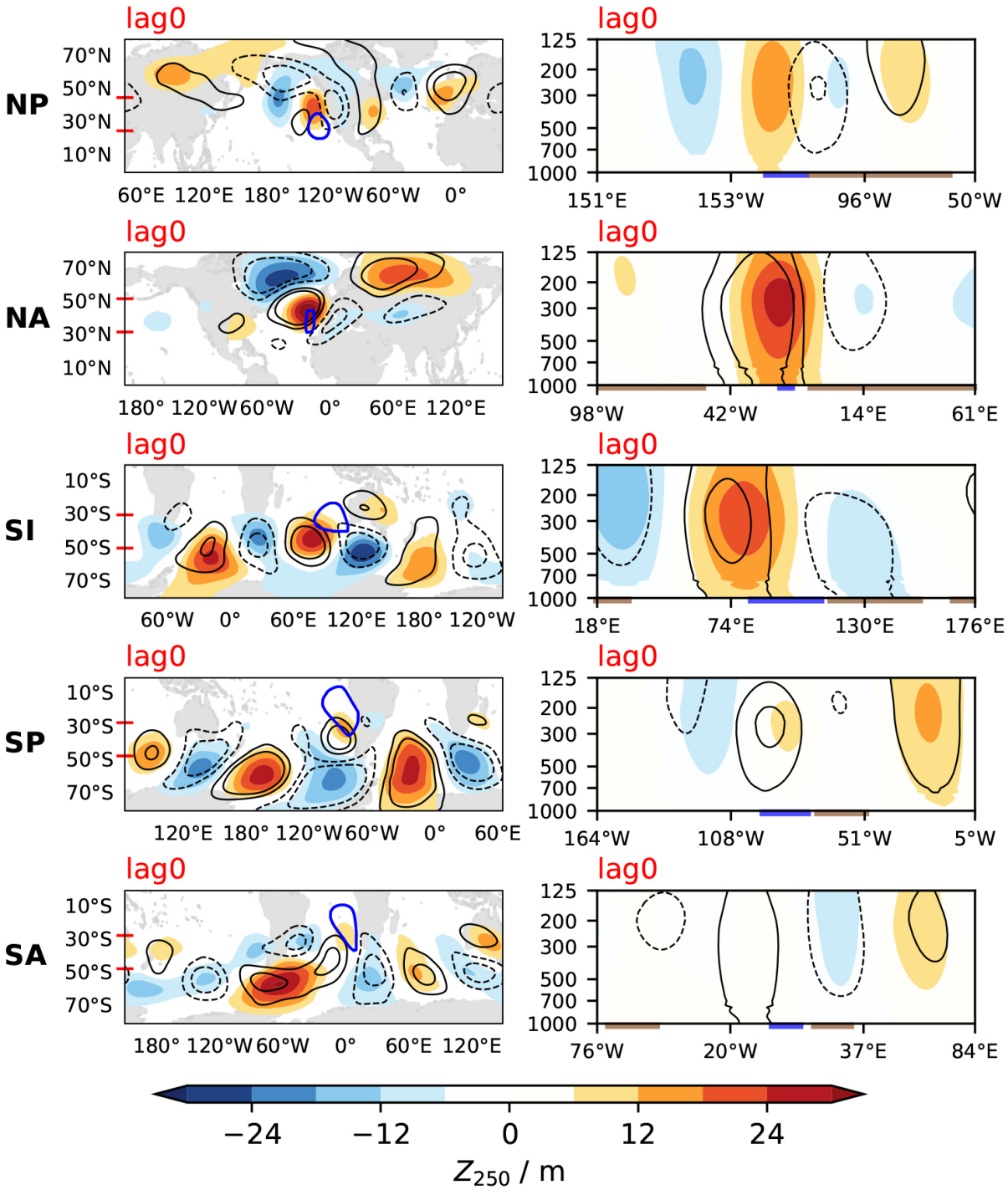

Figure S12: Similar to Figure 5 in the paper but on interseasonal timescales, and only show Rossby modes for all regions.

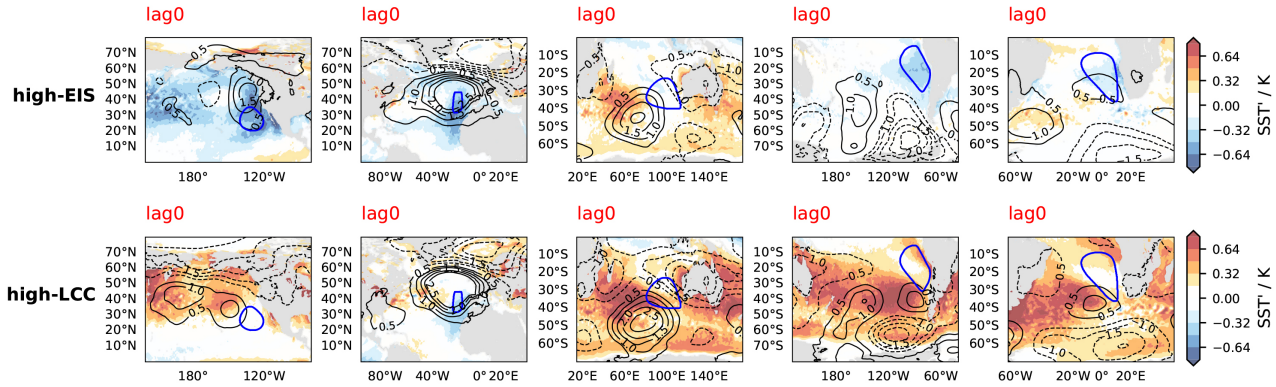

Figure S13: Interseasonal plots for composite high-EIS cases SST and SLP (1st row), and composite high-LCC cases SST and SLP (2nd row). Each column represents one region. The blue thick contour represents Sc areas.

9 Interannual patterns for all regions

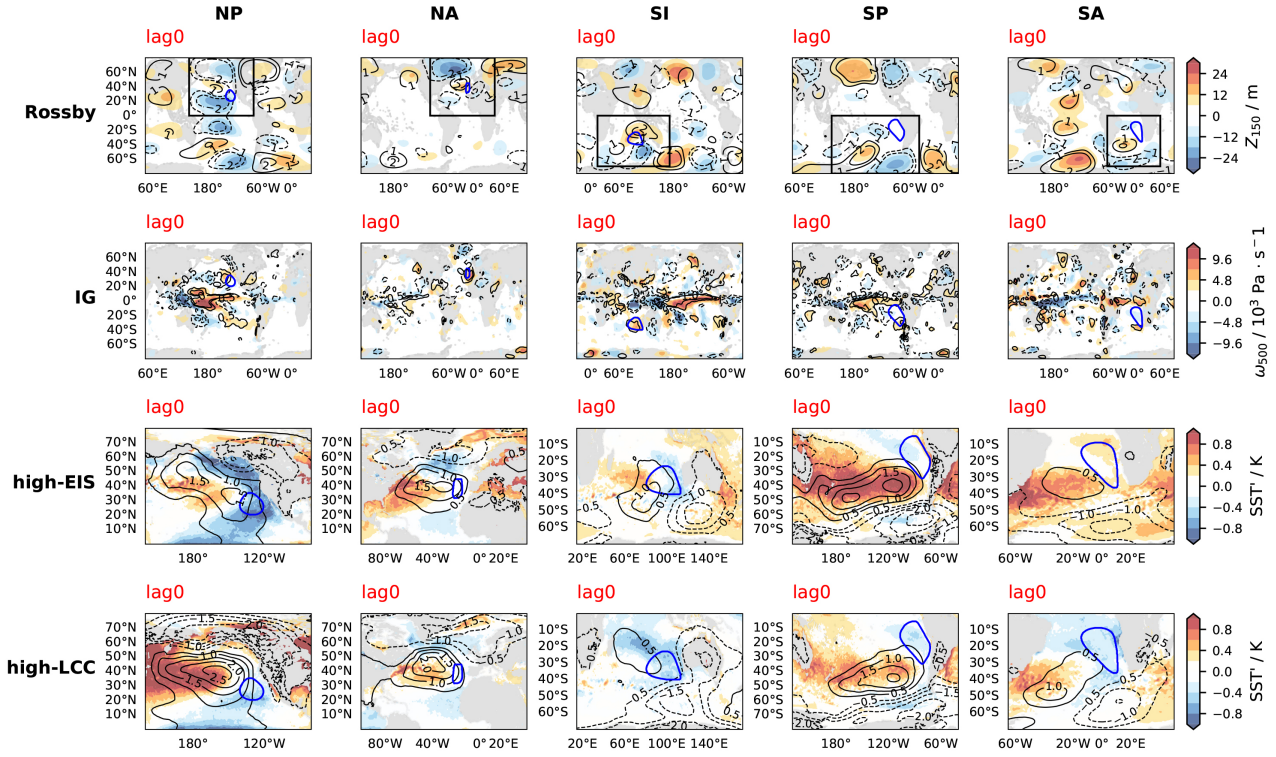

Figure S14: Interannual plots for Rossby modes (1st row), IG modes (2nd row), composite high-EIS cases SST and T_{700} (3rd row), and composite high-LCC cases SST and T_{700} (4th row). Each column represents one region. The black box in the 1st row highlights the plotting domain of the 3rd and 4th rows. The blue thick contour represents Sc areas.

10 The explained variability by extratropical Rossby waves and SST

We quantify the explained variance by the factor of determination R^2 using multi-linear regressions.

- $R^2_{\mathrm{LCC,ucir}}$ (LCC explained by upstream circulation): $\mathrm{LCC} = \alpha + \beta_1\zeta_{250u} + \beta_2 Z_{250u} + \beta_3\mathrm{SST_u} + \varepsilon$;
- $R^2_{\mathrm{EIS,cir}}$ (EIS explained by local circulation): $\mathrm{EIS} = \alpha + \beta_1\zeta_{250} + \beta_2 Z_{250} + \beta_3\mathrm{SST} + \varepsilon$;
- $R^2_{\mathrm{LCC,EIS}}$ (LCC explained by local EIS): $\mathrm{LCC} = \alpha + \beta_1\mathrm{EIS} + \varepsilon$;
- $R^2_{\mathrm{LCC,EIS+ucir}}$ (LCC explained by local EIS and upstream circulation): $\mathrm{LCC} = \alpha + \beta_1\zeta_{250u} + \beta_2 Z_{250u} + \beta_3\mathrm{SST_u} + \beta_4\mathrm{EIS} + \varepsilon$.

where 'u' represents for upstream (box that 10° west and poleward of the respective Sc area), α is the intercept, β_i is the slope coefficient, ζ_{250} is 250 hPa relative vorticity, Z_{250} is 250 hPa geopotential height, and ε is the residual. All factors were standardized by their means and standard deviations before doing regressions.

$$R^2 = 1 - \frac{\mathrm{var}(\varepsilon)}{\mathrm{var}(\mathcal{I})}, \tag{1}$$

where var denotes temporal variance and $\mathcal{I}$ represents the index like LCC or EIS.

Then we adjust R^2 to ensure the comparability among different sets by

$$R^2 = 1 - (1 - R^2)\frac{N-1}{N-p-1}, \tag{2}$$

where N is the length of time series and p is the number of predictors in the multi-linear regression equation.

Results:

Table S2: Coefficients of determination (R^2 / %) from multi-linear regressions. 'orig' denotes the original daily series; 'deseas' denotes the daily series removing the annual cycle.

	orig				deseas			
	$R^2_{\mathrm{LCC,ucir}}$	$R^2_{\mathrm{EIS,cir}}$	$R^2_{\mathrm{LCC,EIS}}$	$R^2_{\mathrm{LCC,EIS+ucir}}$	$R^2_{\mathrm{LCC,ucir}}$	$R^2_{\mathrm{EIS,cir}}$	$R^2_{\mathrm{LCC,EIS}}$	$R^2_{\mathrm{LCC,EIS+ucir}}$
NP	36	70	30	43	17	60	16	24
NA	30	79	26	39	27	76	23	36
SI	20	71	18	28	18	60	27	28
SP	50	79	50	60	11	58	23	29
SA	46	79	44	53	15	49	19	28
Mean	36	76	34	45	18	61	22	29